



Characterization of mortars on the facade of buildings in Gaza-Palestine using experimental techniques

Afonso Rangel Garcez de Azevedo¹ · Markssuel Teixeira Marvila² · Bassam Tayeh³ · Jessica Souza⁴ · Silvio Rainho Teixeira⁵

Received: 18 April 2022 / Revised: 18 July 2022 / Accepted: 24 July 2022 / Published online: 2 August 2022
© The Author(s), under exclusive licence to Springer Nature Switzerland AG 2022

Abstract

The characterization of mortars of facades of buildings located in the Gaza Strip is the main objective of this work. More specifically, the objective of this work is to provide a reliable source of data that allows the documentation of the construction systems used and that serves as a basis for future renovations and interventions in the buildings under study. Three buildings built at different times (Al-Ashi 1920 BC, Al-Ghussain 1865 BC and Al-Hato 1331 BC) were chosen, aiming to evaluate the evolution of the binders used in these buildings. The characterization was performed by chemical mineralogical analysis (XRF), X-ray diffraction spectroscopy (XDR) and Fourier transform infrared spectroscopy (FTIR). The results show that the construction of Al-Ashi consists of mortars made with a natural hydraulic binder obtained with limestone rich in aluminosilicates (clay) and activated by sodium from sea water. Consequently, as the main decomposition phenomena, saline efflorescence was observed. In the realization of the Al-Ghussain building, a natural hydraulic binder was used, made with limestone rock, volcanic ash as natural pozzolans and gypsum plaster to improve the plasticity and adhesion of the mortars. The main pathologies observed were stains and disaggregation, related to the formation of secondary ettringites and mechanical impacts. Finally, the Al-Hato building, built according to Ottoman architecture, features mortars made with natural hydraulic binders like Al-Ghussain and natural fibers. The main pathology is the excess of porous phase, due to the degradation of the natural fiber over time. Thus, it is concluded that the techniques used allow the identification of the main binders used in the production of the mortars under study.

Keywords Historic mortars · Pathology · Characterization · Palestine mortars · Historic facade

✉ Markssuel Teixeira Marvila
markssuel.marvila@ufv.br; markssuel@hotmail.com

Afonso Rangel Garcez de Azevedo
afonso@uenf.br; afonso.garcez91@gmail.com

Bassam Tayeh
bassamtayeh2010@hotmail.com; btayeh@iugaza.edu.ps

Jessica Souza
jessica.souza@unb.br

Silvio Rainho Teixeira
silvio.rainho@unesp.br

¹ LECIV-Civil Engineering Laboratory, UENF-State University of the Northern Rio de Janeiro, 55 (22) 2739-7003; Av. Alberto Lamego, 2000, Campos dos Goytacazes, RJ 28013-602, Brazil

² UFV-Federal University of Viçosa, CRP-Rio Paranaíba Campus; 55 (34) 3855-9000; Rodovia BR 230 KM 7, Rio Paranaíba, MG 38810-000, Brazil

³ Civil Engineering Department, Faculty of Engineering, Islamic University of Gaza, 970 (8) 264 4400, Gaza, Palestine

⁴ UNB-University of Brasília, PECC-Civil and Environmental Engineering Department, Campus Darcy Ribeiro, 55 (61) 3107-3300; Asa Norte, Brasília 70910-900, Brazil

⁵ Faculty of Science and Technology-FCT, Department of Physics, UNESP-São Paulo State University, 55 (18) 3229-5388; Rua Roberto Simonsen, 305, Presidente Prudente, Brazil

1 Introduction

The mortars present on the façades of the buildings are constructive elements that are directly in contact with the aggressive agents of the environment [1]. This is because one of the main functions of these systems is to protect the sealing system and resist thermal actions, in addition to ensuring tightness, fire safety and acoustic insulation and being resistant to wear and surface impacts [2, 3]. These mortars suffer from several pathological problems, among which we can mention: cracks, stains [4], peeling, efflorescence [5, 6], occurrence of fungi and mold [7–9].

These characteristics are aggravated in coastal regions and in regions facing political problems, such as the city of Gaza, located in a region in the Middle East that suffers from many problems related to the stability of construction, mainly due to the large number of regional conflicts [10]. The city of Gaza, for example, has already suffered several bombings that have seriously damaged buildings and their facade systems [11, 12]. On the other hand, this region is known as the cradle of world civilization, bringing together an important architectural ensemble of different buildings from different historical periods [13].

In addition to the reported problems, the city of Gaza is located along a strip of the Mediterranean Sea, being characterized by the arid climate [11, 14]. The city is only 41 km long and between 6 and 12 km wide, totaling an area of approximately 365 km² [15], as shown in Fig. 1. This implies the fact that almost every city is relatively close to the Mediterranean Sea, subject to an intense aggressiveness of chloride salts [16]. Another aggravating factor is the population density, around 5050 inhabitants per km, which provide an intense vehicle traffic on the city's few roads [14, 17]. The city does not have any large industry, and suffers from water scarcity due to the dry and arid climate. All of this information helps in understanding the pathological problems of the mortar of facades of local buildings, and justifies the urgency of technical works that characterize the composition of this material, helping future repairs and restorations [15]. The following are relevant information regarding three buildings located in the city of Gaza, as shown in Fig. 1: the buildings of Al-Ashi, Al-Ghussain and Al-Hato.

1.1 Description of Al-Ashi building

Al-Ashi (Fig. 2) is a building that once functioned as an old public toilet, called Hammam al-Askar, close to the market, built in approximately 1920 BC, subsequently transferred to a housing building, which was abandoned by the owners for some years.



Fig. 1 Location of the buildings studied. Source: A Al-Ashi; B Al-Ghussain and C Al-Hato. N: Geographic north. Source: Aza Strip map

The Al-Ashi building is characterized by an architectural composition that is homogeneous with the local culture prevalent at the time, in addition to its homogeneity with climatic conditions, so that the backyard or internal courtyard that surrounds the house was used, overlooking all the blank spaces. Al-Ashi was chosen for this study because it represents the architecture of the 20th century, with buildings with a more orange color.

Geographically, this building is located in the housing district in the city center, less than 1 km from the Mediterranean Sea. Because it functioned as a public toilet during its early years of foundation, this building was subject to an accelerated degradation, since the humidity coming from the toilets area a strong contrast to the dry and arid climate of the region.

1.2 Description of Al-Ghussain building

The Al-Ghussain building (Fig. 3) is a historical house located in the Al-Daraj neighborhood, Gaza, on Al-Wahda Street, near of the Sabat Al-Alami, being built in 1865 BC to be a residential building. The building has an area of approximately 245 m², representing the classical architecture, which prioritized the lighter and grayish tones, due to influences from other cultures in the region.

Fig. 2 Photos from Al-Ashi building. **a** Surface wear of the inner lining. **b** Internal staircase to access the second floor. **c** Platform for collecting samples. **d** Detail of the external coating of the building. Source: Archive of Islamic University of Gaza



Fig. 3 Photos from Al-Ghussain building. **a** Degradation of the building internal roof. **b** Degradation of the building internal wall. **c, d** External coating of the building and details of degradation. Source: Archive of Islamic University of Gaza



As it is located on one of the main roads in the city of Gaza, the traffic of vehicles is intense in the vicinity, contributing to a high incidence of pollution, causing a degradation in the mortars lining the facades of this building. As it is located approximately 5 km from the oceanic

region, it is impacted by the incidence of the atmosphere of the sea, although in a lower incidence than the Al-Ashi building.

Fig. 4 Photos from Al-Hato building. **a** Arches of the external facade of the building. **b** View of the external facade of the building. **c** Detail of the degradation of the facade and windows. **d** Detail of the degradation of the external facade and access stairs to the second floor. Source: Archive of Islamic University of Gaza



1.3 Description of Al-Hato building.

The Al-Hato building (Fig. 4) is considered one of the houses belonging to the Ottoman era, characterized by large spaces and the use of domes. Built in 1331, with the intense use of natural resources, it illustrates the revolution in construction techniques provided by Ottoman architecture. In 2003, the building underwent a renovation in one of its spaces, but without compromising the building's original architecture.

The Al-Hato building is characterized by the traditional nature of Islamic architecture in the Ottoman era, as it consists of unique architectural elements with a homogeneous shine compatible with local culture and climatic conditions, so he used it in his construction cellars and cross cellars, contracts, arches, yuk and age, in addition to the characteristic decorative elements that indicate the nobility of the building. Located in the region of Deir al-Balah, which characterizes one of the oldest and most upscale neighborhoods in the city of Gaza, it is approximately 6 km from the Mediterranean Sea.

1.4 Research aim

The main objective of this study is to characterize the composition and define the main decay phenomena of the historical mortars on facades located in three buildings in the city of Gaza-Palestine, realized in different historical periods. Specifically, the objective of this manuscript is to provide a reliable source of data that makes it possible to document the construction systems used and to serve as a basis for future renovations and interventions in the buildings under study. Chemical and mineralogical analyses, enabling their knowledge for a possible recovery process, were carried out.

2 Materials and methods

In this study three different buildings were chosen, as highlighted in the introduction: Al-Ashi, Al-Ghussain and Al-Hato. Fig. 5a–c shows the points where the mortar samples of each building were collected. The chosen facade was the one most exposed to the external environment, with a higher



Fig. 5 Sample 1, 2 and 3 collection location: **a** Al-Ashi; **b** Al-Ghusain and **(c)** Al-Hato. Source: Archive of Islamic University of Gaza

index of pathologies, and with the least amount of interventions or reforms, according to information obtained by the building owners. This information is kept in a registry of the Islamic University of Gaza (Faculty of Engineering), which tracks renovations and alterations in these buildings.

The sample extraction procedure followed the recommendations of ISO 2394 [18], using circular samples of approximately 3 cm in diameter, and varying depths. According to ISO 2394 [18] and authors who carried out research with historic buildings [3], the process of taking samples must

be deepened to the point where the old mortar is identified. The process is visual.

For each building, 3 samples were used, extracted from different points of the buildings. According to ISO 2394 [18], the minimum quantity is 3 samples, which need to be taken from points at least 50 cm apart and at most 200 cm apart. This ensures greater uniformity of results. In this research we used the minimum amount of samples. However, as will be noted in the discussion of XRF results, the chemical composition of the extracted samples is very similar, which indicates that the samples are representative.

After collecting the samples, optical microscopy tests were performed using a Jeol microscope model JSM 6460 LV to identify the morphology of historic mortars. Then the samples were disaggregated and transformed into a fine powder, passed through a 200-mesh sieve. The samples in powder form were characterized by X-ray fluorescence, dispersive energy (XRF), in an Axios Max model equipment from the manufacturer Malvern Panalytical operating at 27 kV and 148 mA, with 2 eV resolution. The results were calibrated for the matrix effect, to avoid the re-excitation of atoms by secondary X-rays emitted by neighboring atoms inside the sample. The equipment used presents an SDD detector with a special window made of an ultra-thin film, enabling it to detect ultralight elements such as carbon (C), oxygen (O) and fluorine (F). The characterization was also carried out by X-ray diffraction spectrometry (XRD) for qualitative analysis, using a model 6000 diffractometer from Shimadzu brand, operating with copper radiation ($\text{Cu-K}\alpha$), 40 kV voltage and 2θ sweep ranging from 5° to 70° . Fourier transform infrared spectroscopy (FTIR) tests were also performed using an infrared spectrometer model 4500a and manufacturer Agilent Technologies in the samples in powder form performing transmission in the wavenumber range of $0\text{--}4000\text{ cm}^{-1}$.

3 Results and discussion

3.1 Results for Al-Ashi building

Table 1 presents the results of XRF for the samples studied in the Al-Ashi building. It is observed that in all samples the dominant compositions were SiO_2 , CaO , Na_2O in quantities that total more than 80% of the mortars. It was also possible to detect the presence of Cl , Fe_2O_3 and Al_2O_3 in significant concentrations, and small amounts of MgO . It is known that cement-based mortars have high amounts of CaO , in percentages greater than 60% of the material composition. Thus, the identification of CaO as the second most abundant component is sufficient to realize that Al-Ashi mortars are not predominantly cement-based. In addition, it is observed that the predominant composition is SiO_2 , which

Table 1 Chemical composition by XRF of Al-Ashi mortars (%)

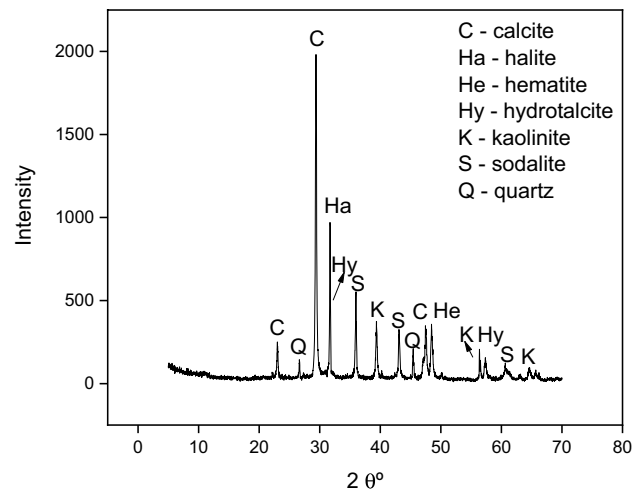
Sample	SiO ₂	CaO	Na ₂ O	Cl	Fe ₂ O ₃	Al ₂ O ₃	MgO	Others
A1	37.23	25.41	24.23	5.85	3.47	2.12	0.74	0.95
A2	33.45	26.12	25.23	4.21	2.14	6.74	0.37	1.74
A3	36.12	25.12	23.67	4.74	3.23	5.45	0.66	1.01

Si silicon, Ca calcium, Na sodium, Cl chlorine, Fe iron, Al aluminium, Mg magnesium, O oxygen

may represent the use of quartz sand. However, it is worth noting that the samples were passed through a 200-mesh aperture sieve before performing the XRF test, reducing the amount of sand particles in the sample. This indicates that the detection of high concentrations of SiO₂ should not be attributed only to the presence of quartz sand. This fact, added to the high contents of Na₂O and Al₂O₃, indicate that the base of the evaluated mortar may be of some activated alkali material (AAM), as is the case of the aluminosilicate based geopolymers. Another possibility is the use of a combination of binder rich in calcium with a rich one and aluminosilicate, due to the percentages of CaO, SiO₂ and Al₂O₃ observed. The presence of Fe₂O₃, on the other hand, is sufficient to explain the orange coloration observed in the mortars of Fig. 2. This characteristic reinforces the possibility of using AAM in Al-Ashi mortars.

Also noteworthy is the presence of Cl, in quantities around 4–6%, which is a considerable content. This may suggest the deposition of salts from the Mediterranean Sea. The Al-Ashi building is located in the direct zone of contact with the sea, about 1 km from the ocean coast. This suggests that the Cl present in the composition of the mortars comes from this source. In addition, the use of coastal sand cannot be ruled out as a probable source of Cl found in mortars [19]. However, as will be discussed in the sequence of the text, the mortars of the Al-Ghussai and Al-Hato buildings do not have levels of Cl found in their chemical compositions, even though they are relatively close to the sea (between 5 and 6 km away). This suggests the intentional inclusion of chlorides in the composition of mortars. This information suggests, therefore, the use of sea water, rich in sodium and chlorine, as a component of mortars for the alkaline activation process, which is a practice reported by other researchers in historic mortars [20, 21].

Figure 6 shows the XRD results for Al-Ashi mortar samples. The results presented correspond to sample 1, to avoid excessive information in the figures. The main minerals identified in Fig. 6 are also shown in Table 2. Figure 6 and Table 2 shows the presence of sodalite, a typical mineral of the alkaline activation of binders rich in aluminosilicates that originate geopolymers [22]. It is also possible to identify the presence of kaolinite in the sample. This suggests that the mortars in the region were produced using clay from the region, known to be kaolinite [16, 23], as a binder, responsible for the formation of sodalite minerals after alkaline

**Fig. 6** XRD analysis of Al-Ashi mortar

activation. In Fig. 6 it is also possible to identify the presence of hydrotalcite and calcite minerals. This information indicates that, in addition to kaolinite clay, it was used in the limestone found in the region as binders. This probably led to the formation of hydrotalcite identified in the XRD. This mineral is a hydrated calcium aluminate, it presents in the alkaline activation of calcium rich binders [24, 25], such as limestone, in the presence of aluminate phases, from the use of kaolinitic clay [26]. It is further evidence of the use of the principles of alkaline activation for the production of Al-Ashi mortars. Thus, it is observed that the mortars in the region were probably produced through the use of kaolinitic clay and limestone as a binder. Limestone deposits are abundant in the region, and justify the presence of calcite in this composition [27]. There was the presence of hematite in the clay, responsible for the reddish coloring of the mortars, as it is detected in Fig. 6. In addition, the presence of quartz was detected, probably used in the mortars as fine aggregate or present as impurity in the clay and limestone. It was also possible to detect halite, showing the occurrence of chlorine in the material. The chlorine most likely comes from sea water, a possible material used as an activating solution for the alkaline activation reaction that originated the mortars in the region. The use of salt as an alkaline activated in historic mortars has been proven by other authors [20, 28].

Table 2 Minerals identified by the XRD of mortars from Al-Ashi

Mineral	Probable origin
Calcite	Use of limestone as binders or binders rich in calcium
Halite	Use of sea water as an alkaline activator, or attack of chlorides in the coastal region
Hematite	Use of clays with iron oxide, responsible for the reddish color
Hydrotalcite	Typical mineral obtained from the alkaline activation of binders rich in calcium, such as limestone
Kaolinite	Use of clays as binders or binders rich in aluminosilicates
Sodalite	Typical mineral obtained from the alkaline activation of binders rich in aluminosilicates, such as kaolinitic clay
Quartz	Use of sand as aggregates

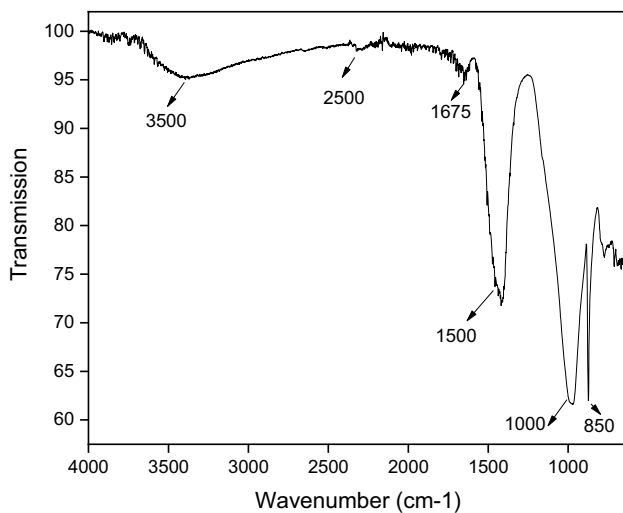
**Fig. 7** FTIR analysis of Al-Ashi mortar

Figure 7 shows the FTIR results for sample 1 of Al-Ashi. A first event is observed at 3500 cm^{-1} , related to the water of constitution of mortars, and vibration of O–H bonds. The event that occurs at 1675 cm^{-1} is also related to the vibration of the O–H bonds of the constitution water [29]. The small event that occurs in 2500 cm^{-1} is associated with the Ca–H bond, typical of calcium-rich binders, such as limestone [30]. The events at 1500 , 1000 and 850 cm^{-1} are typical of activated alkali materials, as they are related, respectively, to the vibration of the sodium phases, the Si–O–Si bond, and the Si–Ca–Si bond [30, 31]. This information proves that the Al-Ashi mortar base is materials activated alkaline using a solution rich in sodium and with a mixture of binders rich in calcium and aluminosilicates. This proves the discussion held by the XRD analysis.

Figure 8 shows the microscopy of the Al-Ashi mortar samples. Figure 8a shows the occurrence of efflorescence on the mortar surface. This type of problem is the main pathological defect found in activated alkali materials, which is the likely composition of Al-Ashi mortars. In addition, Fig. 8b shows the occurrence of porosity, a characteristic

practically impossible to remove from mortars, and an irregular surface, typical of old mortars. Figure 8c shows the XRD of the efflorescence powder illustrated in Fig. 8a. The presence of natron ($\text{Na}_2\text{CO}_3 \cdot 7\text{H}_2\text{O}$) is observed in the efflorescence powder, which is the main constituent of efflorescence of activated alkali materials [32, 33].

3.2 Results for Al-Ghussain building

Table 3 presents the results of XRF for the samples studied in the Al-Ghussain building. There is a predominance of CaO, followed by smaller amounts of SiO_2 , Fe_2O_3 and Al_2O_3 . It is also worth highlighting the presence of SO_3 and MgO. The composition observed for Al-Ghussain mortars is typical of natural binders-based materials, where the structures formed after hydration are silicate-calcium and ferroaluminate-calcium [34], obtained by mixing limestone rock with natural pozzolanas, such as volcanic ash. Thus, the presence of high levels of CaO (> 80%) is related to the use of limestone, which presents in its composition small amounts of MgO (between 0.5 and 0.7%) [35]. The presence of SiO_2 , Al_2O_3 , and Fe_2O_3 is attributed to the use of volcanic ash, very common in this region of Asia, as highlighted by other authors [36, 37]. The presence of SO_3 is attributed to the use of gypsum plaster, mixed together with the other components of the mortar in the form of powder and necessary to improve the plasticity and adhesion properties of the material [3, 38].

Figure 9 and Table 4, which presents the XRD results for Al-Ghussain's sample 1, confirms the information observed in Table 3. The formation of C–S–H (calcium silicate hydrate), secondary ettringite and portlandite (calcium hydroxides) minerals, typical of natural hydraulic binders hydration, is verified [34, 35]. In addition to these minerals, the presence of quartz is observed, probably due to the use of sand as aggregate, and calcite probably from limestone. No peaks related to the dolomite mineral are detected, due to the low amount of MgO observed in the composition, which suggests that the limestone used is predominantly based in calcite. The presence of this last

Fig. 8 Microscopy of Al-Ashi mortars: **a** efflorescence; **b** external surface; **c** XRD of efflorescence

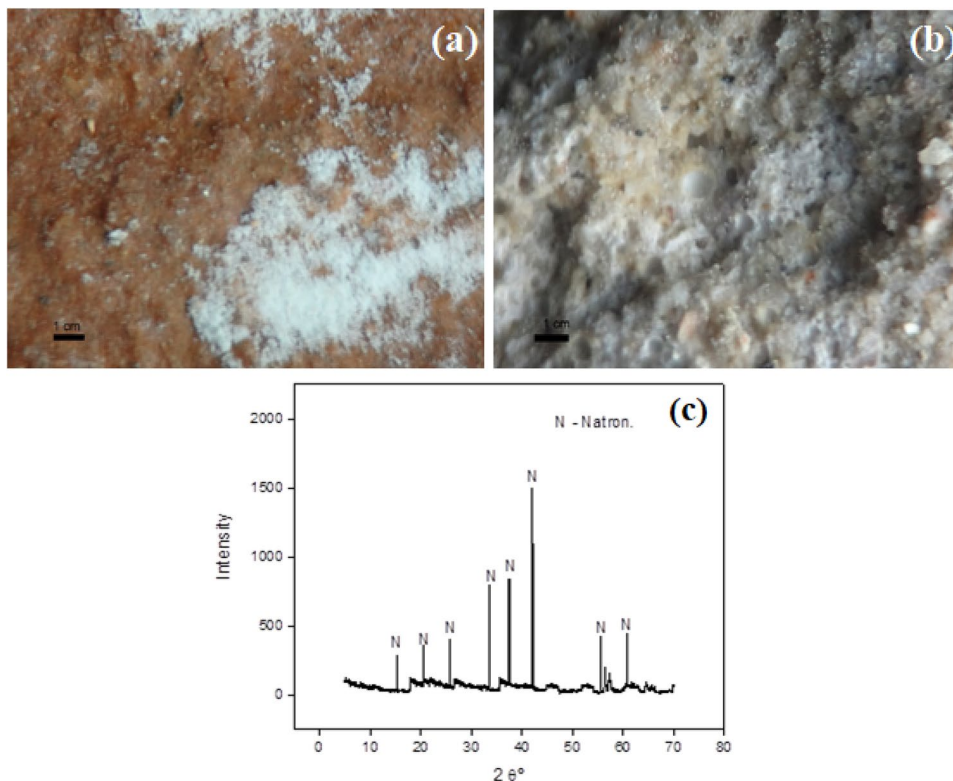


Table 3 Chemical composition by XRF of Al-Ghussain mortars (%)

Sample	CaO	SiO ₂	Fe ₂ O ₃	Al ₂ O ₃	SO ₃	MgO	Others
G1	82.65	7.76	3.45	2.37	1.47	0.56	1.74
G2	80.33	8.12	3.57	2.33	1.55	0.67	3.43
G3	81.26	7.68	3.23	3.89	1.31	0.49	2.14

Ca calcium, Si silicon, Fe iron, Al aluminum, S sulfur, Mg magnesium, O oxygen

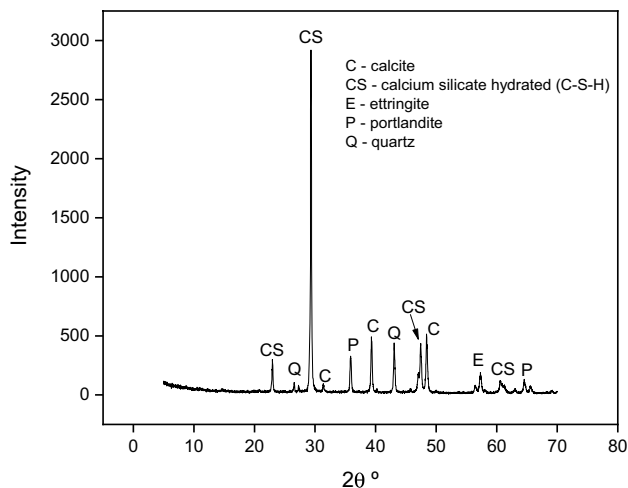


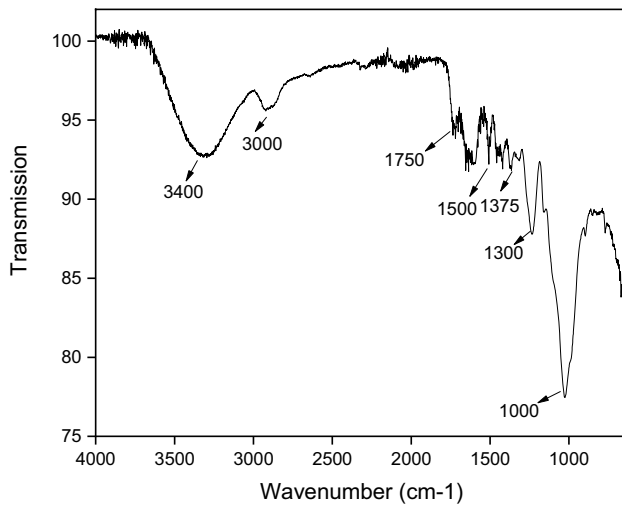
Fig. 9 XRD analysis of Al-Ghussain mortar

mineral suggests that the natural hydraulic binders used to manufacture mortars was not fully reactive, which can be attributed to the lower technology available at the time the building was built (1865 BC). Knowledge about OPC was not fully established at that time, an indication that the natural hydraulic binders used in manufacturing was a simpler type, probably inspired by Roman cements [21, 39]. This material was produced using natural pozzolans, such as volcanic ash or ash from agricultural processes, and limestone rock [40, 41]. Probably the natural hydraulic binders used in the production of mortars has a similar composition.

It is observed in Fig. 9 and Table 4 that the ettringite present in mortars is secondary, not primary. It is known that the primary ettringite is formed soon after the hydration of the natural hydraulic binders, and that it disappears

Table 4 Minerals identified by the XRD of mortars from Al-Ghussain

Mineral	Probable origin
Calcite	Limestone used for the production of the natural hydraulic binders
C–S–H	Main hydration product of the natural hydraulic binders
Ettringite	Formed due to external agents, such as sulfates
Portlandite	Secondary hydration product of the natural hydraulic binders
Quartz	Use of sand as aggregates

**Fig. 10** FTIR analysis of Al-Ghussain mortar

with the course of the reaction time [42]. However, secondary ettringite, which can originate in two different ways, remains in the natural hydraulic binders composition even after years of its formation [43, 44]. The first way that secondary ettringite can be formed is due to inhibition of the reaction or thermal decomposition of the primary ettringite by excess heat. In this way, when the mortar cools down, the secondary interlayer will form with the material already hardened, generating internal stresses superior to the mortar's tensile strength [45]. Another case that causes the formation of this type of ettringite is due to external agents, usually sulfate attack, more likely to

have occurred in the case of the mortars studied in this work [44, 46]. The source of sulphate attack is related to environmental pollution from gases emitted by vehicles, since the region where Al-Ghussain building is close to Al-Wahda Street, one of the main streets in Gaza. In this circumstance, the formation of secondary ettringite is related to the conversion of monosulfoaluminate back to ettringite, due to the entry of SO_4 ions into the cementitious environment, causing stresses that cause cracks in the hardened mortar [42, 43]. The occurrence of secondary ettringite was verified by other authors who studied Roman cement [47], a binder similar to that used in Al-Ghussain building mortars.

Figure 10 shows the FTIR results of Al-Ghussain mortars from sample 1. The event that occurs at 3400 cm^{-1} is related to the O–H connections, of the water used to form mortars [48]. The event that occurs at 3000 cm^{-1} is related to the presence of portlandite, characterized by Ca–H bonds, as well as the event related to 1500 cm^{-1} [49]. The event that occurs at 1750 cm^{-1} is related to the vibrations of the C–S–H bonds, indicating the presence of this phase in the material. The 1300 and 1000 cm^{-1} events are also related to C–S–H [49, 50]. It is still worth highlighting the event that occurs at 1375 cm^{-1} , attributed to the bonds of the carbonate phases, that is, CaCO_3 present in the limestone rock [50]. FTIR analysis shows the results obtained by XRD, that Al-Ghussain mortars are typically cementitious, but with a material with less reactivity than OPC, with the presence of limestone being observed in the composition. This material is a natural hydraulic binder.

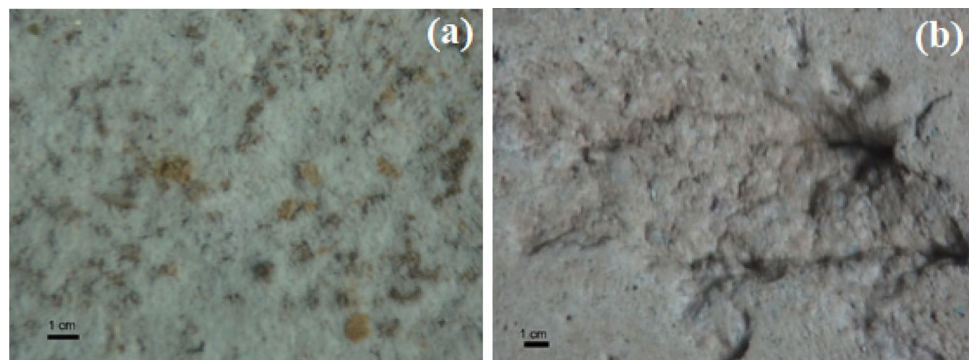
Fig. 11 Microscopy of Al-Ghussain mortars: **a** stains; **b** external surface

Table 5 Chemical composition by XRF of Al-Hato mortars (%)

Sample	CaO	SiO ₂	C	Fe ₂ O ₃	Al ₂ O ₃	SO ₃	MgO	Others
H1	55.12	18.27	13.55	4.22	4.69	2.61	0.63	0.91
H2	52.74	20.08	14.37	5.57	4.75	1.21	0.39	0.89
H3	54.63	17.75	10.88	6.41	5.12	2.33	0.53	2.35

Ca calcium, Si silicon, C carbon, Fe iron, Al aluminium, S sulfur, Mg magnesium, O oxygen

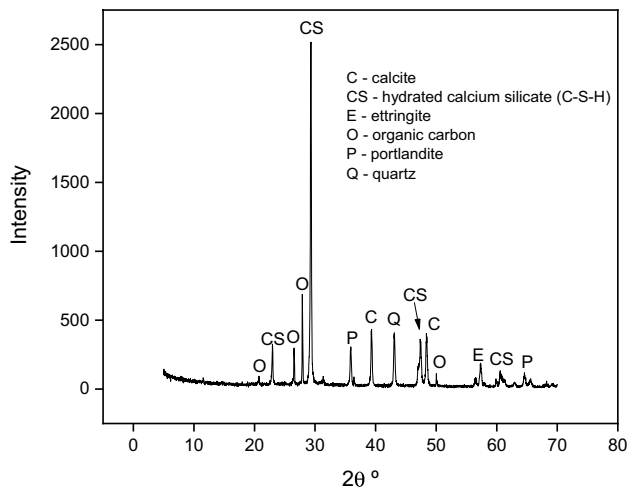


Fig. 12 XRD analysis of Al-Hito mortar

Figure 11a shows the whitish aspect of mortar, typical of the classical architectural period represented by Al-Ghussain. Figure 11a also shows the presence of yellowish spots, which can be associated with the concentration of another phase other than the natural hydraulic binder used. This phase is considered a pathological problem because it compromises the aesthetics of the mortar, giving an aspect of stains in the material. Figure 11b shows the irregularity on the external surface of the material, related to the loss of mass presented by the mortars. This loss of mass can be attributed to the formation of expansive secondary ettringite, given the contents of the material detected in Figure 9, or due to mechanical impacts on the material.

3.3 Results for Al-Hato building

Table 5 presents the results of XRF for the samples studied in the Al-Hato building. It is observed that the composition of mortars is predominantly CaO and SiO₂, with high amounts of C. Significant concentrations of Fe₂O₃, Al₂O₃, SO₃ and smaller amounts of MgO are also found. It is observed that the chemical composition of the mortars indicates that the material is probably formed from natural hydraulic binders, due to the high concentrations of CaO, SiO₂, Fe₂O₃, Al₂O₃ and SO₃ [34, 35] similar to Al-Ghussain mortars. On the other hand, the presence of C in the composition of mortars, indicates the introduction of an organic phase, attributed to the inclusion of natural fibers [51], a common practice during the Ottoman era, due to the domed buildings that introduced tensile efforts in the construction components.

Figure 12 shows the XRD results for sample 1 of Al-Hato. These results are also summarized in Table 6. The presence of C–S–H, portlandite and secondary ettringite was observed, due to the hydration of the natural hydraulic binders [34, 35]. In addition, there is the presence of calcite, a mineral typical of limestone that was used in the production of hydraulic natural binders used in constructions in the region [27]. In addition, it is possible to observe the presence of organic carbon, related to the introduction of natural fibers [52]. This information proves the information highlighted in Tables 5 and 6. Regarding natural fibers, there are indications that Ottoman architecture incorporated animal fibers found in the region in the building components. The fibers of rabbits, foxes, deer and rodents stand out, like related by others authors [51–53]. The fibers are used to increase the tensile strength of mortars, necessary due to the geometry of buildings from the Ottoman era. The use of

Table 6 Minerals identified by the XRD of mortars from Al-Hito

Mineral	Probable origin
Calcite	Limestone used for the production of the natural hydraulic binders
C–S–H	Main hydration product of the natural hydraulic binders
Secondary ettringite	Formed due to external agents, such as sulfates
Organic carbon	From natural fibers
Portlandite	Secondary hydration product of the natural hydraulic binders
Quartz	Use of sand as aggregates

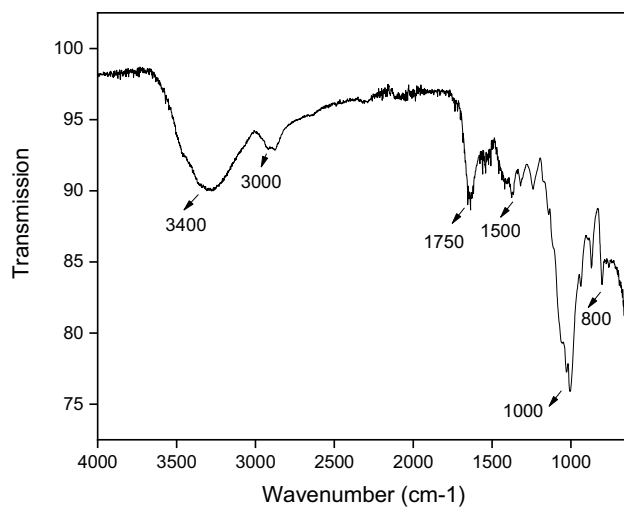


Fig. 13 FTIR analysis of Al-Hito mortar

fibers does not affect the hydraulicity of the natural hydraulic binders used in the composition of these mortars.

Figure 13 shows the FTIR analysis for sample 1 of Al-Hato mortars. The same events described in the analysis of Fig. 8 are observed, which reported the FTIR of the sample from Al-Ghussain. This is an indication that the basic raw material used to produce the natural hydraulic mortar in the region is similar, probably from the same limestone deposits. Although the events observed in 3400 cm^{-1} (constitution water), 3000 and 1500 cm^{-1} (portlandite), 1750 and 1000 cm^{-1} (CSH) [49, 50], the events observed by Al-Ghussain mortars are equivalent, it is valid to point out that there is an event in 800 cm^{-1} exclusive to Al-Hito mortars. This event can be attributed to the decomposition of C–C bonds, indicating the presence of organic matter [54, 55], linked to the use of natural fibers in the region's mortars. This proves the results discussed by the XRD analysis.

Figure 14 shows the microscopy of Al-Hato mortars. It is possible to identify the excess of porous phase in the material, which can occur due to weathering, and also the presence of quartz particles. Another important information

observed in the figure is the presence of darker regions, in addition to particles of dots with the same coloring. This characteristic can be attributed to the presence of vegetable fibers in the composition of the mortar, as previously reported.

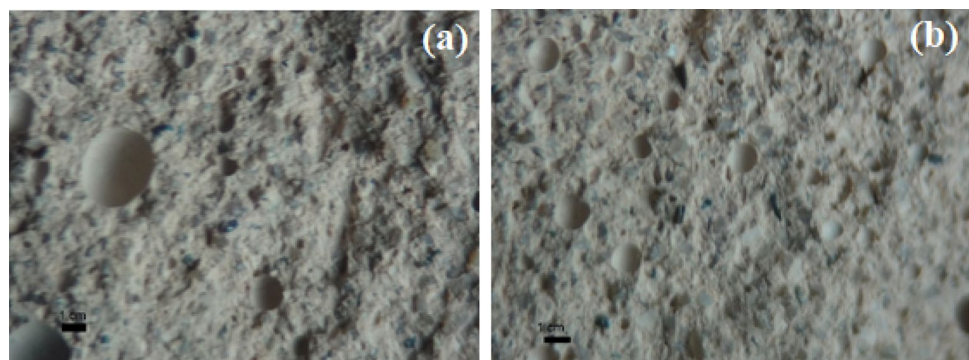
4 Conclusion

The aim of this work was to characterize, identify the composition and main pathologies of historic mortars in buildings located in Gaza-Palestine, in order to provide a reliable database for documenting the buildings studied and to serve as a basis for future renovations. Microscopy, XRF, XRD and FTIR techniques were used in three different buildings.

It is concluded that Al-Ashi mortars, dating from 1920 BC representing of architecture of the 20th century, are produced based on kaolinitic clay with iron and limestone activated alkaline with sea water in the region. This information is compatible with the chemical and mineralogical composition of the samples, which contain kaolinite and hematite from the clay and calcite from the limestone used as binders. In addition, there is a high content of Cl in the chemical composition, originated from the saline attack, since this building is approximately 1 km from the sea, but also due to the use of sea water in alkaline activation. The minerals of sodalite and hydrotalcite, main products of alkaline activation, were identified in the analysis of XRD and FTIR. This confirms the alkaline activation of the Al-Ashi mortars. The main pathologies identified were efflorescence, confirmed by microscopic analysis and by XRD.

Al-Ghussain mortars, from 1865 BC, represent the classic model and were produced using limestone, volcanic ash like natural pozzolana and gypsum plaster for production of natural hydraulic binders, with less reactivity than Portland cement. This information was confirmed by the chemical and mineralogical composition, where it was detected the presence of C–S–H, portlandite, secondary ettringite, in addition to calcite that suggest that the natural

Fig. 14 Microscopy of Al-Hato mortars: **a** and **b** surface of the material



hydraulic binder used was not fully reactive. In addition, the formation of secondary ettringite, motivated by the attack of sulfates, can be considered the main pathology of this system, producing loss of mass and breakdowns.

Finally, it is concluded that Al-Hato mortars, dating from 1331 BC from the Ottoman period, are characterized by being the natural hydraulic binders base with the introduction of natural fibers, of the animals present in the region. This characteristic was essential to improve the required tensile strength due to the architectural details of the Ottoman model. This information was proven using the techniques of XRF, XRD and FTIR, where in addition to the typical compounds of natural hydraulic binders, the presence of organic matter was also observed. The main pathology detected was excess formation of porous phase, attributed to the wear of the natural fiber over time.

Based on the results obtained, consistent with other published research, it can be concluded that these are preliminary data that must be implemented, nevertheless they give an idea of the characteristics of the mortars and their state of conservation. As discussed in the introduction, the region where the buildings are located is of great importance to the history of humanity. On the other hand, they are located in an area of difficult access due to regional conflicts. As a result, the results of the article are useful because they explore buildings in a region that have not yet been fully studied and published in scientific articles. In addition, the results present an interesting and simple methodology, which can be applied to other similar studies. These are the main contributions of the present work.

Author contribution All authors contributed to the study conception and design. Material preparation, data collection and analysis were performed by AA, JS, SR and BT. The first draft of the manuscript was written by MM and AA and all authors commented on previous versions of the manuscript. All authors read and approved the final manuscript.

Funding The authors declare that no funds, grants, or other support were received during the preparation of this manuscript.

Declarations

Ethical approval This research does not involve the need for ethics approval.

Conflict of interest The authors declare that there are no conflicts of interest. The authors have no relevant financial or non-financial interests to disclose.

Informed consent Informed consent was obtained from all individual participants included in the study.

References

- Vega-Garcia P, Schwerd R, Scherer C et al (2020) Influence of façade orientation on the leaching of biocides from building façades covered with mortars and plasters. *Sci Total Environ*. <https://doi.org/10.1016/j.scitotenv.2020.139465>
- Pereira C, de Brito J, Silvestre JD (2020) Harmonising the classification of diagnosis methods within a global building inspection system: proposed methodology and analysis of fieldwork data. *Eng Fail Anal*. <https://doi.org/10.1016/j.engfailanal.2020.104627>
- Marvila MT, Azevedo ARG, Barroso LS et al (2020) Gypsum plaster using rock waste: a proposal to repair the renderings of historical buildings in Brazil. *Constr Build Mater* 250:118786. <https://doi.org/10.1016/j.conbuildmat.2020.118786>
- Carretero-Ayuso MJ, Sáez-Pérez MP (2021) Construction flaws in facing brick facades and the risk of associated litigation. *J Build Eng* 33:101633. <https://doi.org/10.1016/j.jobe.2020.101633>
- Barreiras J, de Brito J, Correia JR (2016) Analysis of the degradation condition of secondary schools. Case study: pavilions and prefabricated buildings. *J Civ Eng Manag*. <https://doi.org/10.3846/13923730.2014.914090>
- Azevedo ARG, Marvila MT, Rocha HA et al (2020) Use of glass polishing waste in the development of ecological ceramic roof tiles by the geopolymerization process. *Int J Appl Ceram Technol* 17:2649–2658. <https://doi.org/10.1111/ijac.13585>
- Diaz C, Cornadó C, Albareda A (2020) Damage in face-brick facades placed between concrete slabs. *J Build Eng* 30:101312. <https://doi.org/10.1016/j.jobe.2020.101312>
- Salomão de MCF, Bauer E, Kazmierczak de CS (2018) Drying parameters of rendering mortars. *Amb Const*. <https://doi.org/10.1590/s1678-86212018000200239>
- Sá G, Sá J, De Brito J, Amaro B (2015) Statistical survey on inspection, diagnosis and repair of wall renderings. *J Civ Eng Manag*. <https://doi.org/10.3846/13923730.2014.890666>
- (2010) Building for the future: overview of the Middle East paints and coatings industry. *Focus Powder Coatings*. [https://doi.org/10.1016/s1364-5439\(10\)70151-9](https://doi.org/10.1016/s1364-5439(10)70151-9)
- Slitine M (2018) Contemporary art from a city at war: the case of Gaza (Palestine). *Cities*. <https://doi.org/10.1016/j.cities.2017.11.010>
- Asfour OS, Zourob N (2017) The neighbourhood unit adequacy: an analysis of the case of Gaza, Palestine. *Cities* 69:1–11. <https://doi.org/10.1016/j.cities.2017.05.014>
- Sameeh El halabi A, ElSayad ZT, Ayad HM (2019) VRGIS as assistance tool for urban decision making. *Alexandria Eng J* 58:367–375. <https://doi.org/10.1016/j.aej.2018.07.016>
- Fathi Nassar Y, Yassin Alsadi S (2019) Assessment of solar energy potential in Gaza Strip-Palestine. *Sustain Energy Technol Assess* 31:318–328. <https://doi.org/10.1016/j.seta.2018.12.010>
- Manduca P, Al Baraqui N, Al Baraqui L et al (2019) Hospital centered surveillance of births in Gaza, Palestine, 2011–2017 and heavy metal contamination of the mothers reveals long-term impact of wars. *Reprod Toxicol* 86:23–32. <https://doi.org/10.1016/j.reprotox.2019.02.003>
- Abu Al Naeem MF, Yusoff I, Ng TF et al (2019) A study on the impact of anthropogenic and geogenic factors on groundwater salinization and seawater intrusion in Gaza coastal aquifer, Palestine: an integrated multi-techniques approach. *J Afr Earth Sci* 156:75–93. <https://doi.org/10.1016/j.jafrearsci.2019.05.006>
- Abushab KM, Suleiman MD, Alajerami YSM et al (2018) Evaluation of advanced medical imaging services at Governmental Hospitals-Gaza Governorates, Palestine. *J Radiat Res Appl Sci* 11:43–48. <https://doi.org/10.1016/j.jrras.2017.10.007>
- ISO (2015) ISO 2394:2015—General Principles on Reliability for Structures. *Int Organ Stand*

19. Borges C, Santos Silva A, Veiga R (2014) Durability of ancient lime mortars in humid environment. *Constr Build Mater* 66:606–620. <https://doi.org/10.1016/j.conbuildmat.2014.05.019>
20. Divya Rani S, Rahul AV, Santhanam M (2021) A multi-analytical approach for pore structure assessment in historic lime mortars. *Constr Build Mater* 272:121905. <https://doi.org/10.1016/j.conbuildmat.2020.121905>
21. Oliveira MLS, Flores EMM, Dotto GL et al (2021) Nanomineralogy of mortars and ceramics from the Forum of Caesar and Nerva (Rome, Italy): the protagonist of black crusts produced on historic buildings. *J Clean Prod* 278:123982. <https://doi.org/10.1016/j.jclepro.2020.123982>
22. Fořt J, Novotný R, Vejmelková E et al (2019) Characterization of geopolymers prepared using powdered brick. *J Mater Res Technol* 8:6253–6261. <https://doi.org/10.1016/j.jmrt.2019.10.019>
23. Sandler A, Herut B (2000) Composition of clays along the continental shelf off Israel: contribution of the Nile versus local sources. *Mar Geol* 167:339–354. [https://doi.org/10.1016/S0025-3227\(00\)00021-9](https://doi.org/10.1016/S0025-3227(00)00021-9)
24. Erfanimanesh A, Sharbatdar MK (2020) Mechanical and microstructural characteristics of geopolymer paste, mortar, and concrete containing local zeolite and slag activated by sodium carbonate. *J Build Eng* 32:101781. <https://doi.org/10.1016/j.job.2020.101781>
25. Papa E, Medri V, Paillard C et al (2019) Geopolymer-hydratolite composites for CO₂ capture. *J Clean Prod* 237:117738. <https://doi.org/10.1016/j.jclepro.2019.117738>
26. Aziz A, Stocker O, El Amrani El Hassani I-E et al (2021) Effect of blast-furnace slag on physicochemical properties of pozzolan-based geopolymers. *Mater Chem Phys* 258:123880. <https://doi.org/10.1016/j.matchemphys.2020.123880>
27. Abu alnaeem M, Yusoff I, Ng T et al (2019) An integrated multi-techniques approach for hydrogeochemical evaluation of ion exchange processes and identification of water types based on statistical analysis: application to the Gaza coastal aquifer, Gaza Strip. *Palestine Groundw Sustain Dev* 9:100227. <https://doi.org/10.1016/j.gsd.2019.100227>
28. Li Y-L, Zhao X-L, Singh Raman RK, Al-Saadi S (2018) Thermal and mechanical properties of alkali-activated slag paste, mortar and concrete utilising seawater and sea sand. *Constr Build Mater* 159:704–724. <https://doi.org/10.1016/j.conbuildmat.2017.10.104>
29. Ma H, Tian Y, Li Z (2011) Interactions between organic and inorganic phases in PA- and PU/PA-modified-cement-based materials. *J Mater Civ Eng* 23:1412–1421. [https://doi.org/10.1061/\(ASCE\)MT.1943-5533.0000302](https://doi.org/10.1061/(ASCE)MT.1943-5533.0000302)
30. Toniolo N, Taveri G, Hurle K, Ercole P, Dlouhy I (2017) Fly-ash-based geopolymers: how the addition of recycled glass or red mud waste influences the structural and mechanical properties. *J Ceram Sci Technol* 08:411–420. <https://doi.org/10.4416/JCST2017-00053>
31. Kumar S, Kristály F, Mucsi G (2015) Geopolymerisation behaviour of size fractionated fly ash. *Adv Powder Technol* 26:24–30. <https://doi.org/10.1016/j.apt.2014.09.001>
32. Zhang Z, Provis JL, Reid A, Wang H (2014) Fly ash-based geopolymers: the relationship between composition, pore structure and efflorescence. *Cem Concr Res* 64:30–41. <https://doi.org/10.1016/j.cemconres.2014.06.004>
33. Temuujin J, van Riessen A, Williams R (2009) Influence of calcium compounds on the mechanical properties of fly ash geopolymer pastes. *J Hazard Mater* 167:82–88. <https://doi.org/10.1016/j.jhazmat.2008.12.121>
34. Loureiro AMS, Paz SPA, Veigado MR, Angélica RS (2020) Assessment of compatibility between historic mortars and lime-METAKAOLIN restoration mortars made from amazon industrial waste. *Appl Clay Sci* 198:105843. <https://doi.org/10.1016/j.clay.2020.105843>
35. Taglieri G, Daniele V, Rosatelli G et al (2017) Eco-compatible protective treatments on an Italian historic mortar (XIV century). *J Cult Herit* 25:135–141. <https://doi.org/10.1016/j.culher.2016.12.008>
36. Zeyad AM, Khan AH, Tayeh BA (2020) Durability and strength characteristics of high-strength concrete incorporated with volcanic pumice powder and polypropylene fibers. *J Mater Res Technol* 9:806–818. <https://doi.org/10.1016/j.jmrt.2019.11.021>
37. Zeyad AM, Tayeh BA, Yusuf MO (2019) Strength and transport characteristics of volcanic pumice powder based high strength concrete. *Constr Build Mater* 216:314–324. <https://doi.org/10.1016/j.conbuildmat.2019.05.026>
38. Pintér F, Vidovszky I, Weber J, Bayer K (2014) Mineralogical and microstructural characteristics of historic Roman cement renders from Budapest, Hungary. *J Cult Herit* 15:219–226. <https://doi.org/10.1016/j.culher.2013.04.007>
39. Klisińska-Kopacz A, Tišlova R, Adamski G, Kozłowski R (2010) Pore structure of historic and repair Roman cement mortars to establish their compatibility. *J Cult Herit* 11:404–410. <https://doi.org/10.1016/j.culher.2010.03.002>
40. Kirilovica I, Vitina I, Grase L (2021) Structural investigation of carbonation and hydration process of hydraulic dolomitic binder. *Constr Build Mater* 275:122050. <https://doi.org/10.1016/j.conbuildmat.2020.122050>
41. Secco M, Previato C, Addis A et al (2019) Mineralogical clustering of the structural mortars from the Sarno Baths, Pompeii: a tool to interpret construction techniques and relative chronologies. *J Cult Herit* 40:265–273. <https://doi.org/10.1016/j.culher.2019.04.016>
42. Wang A, Zheng Y, Zhang Z et al (2020) The durability of alkali-activated materials in comparison with ordinary portland cements and concretes: a review. *Engineering* 6:695–706. <https://doi.org/10.1016/j.eng.2019.08.019>
43. Selim FA, Hashem FS, Amin MS (2020) Mechanical, microstructural and acid resistance aspects of improved hardened Portland cement pastes incorporating marble dust and fine kaolinite sand. *Constr Build Mater* 251:118992. <https://doi.org/10.1016/j.conbuildmat.2020.118992>
44. Nguyen H, Kunther W, Gijbels K et al (2021) On the retardation mechanisms of citric acid in ettringite-based binders. *Cem Concr Res* 140:106315. <https://doi.org/10.1016/j.cemconres.2020.106315>
45. e Silva RA, de Castro Guetti P, da Luz MS, et al (2017) Enhanced properties of cement mortars with multilayer graphene nanoparticles. *Constr Build Mater* 149:378–385. <https://doi.org/10.1016/j.conbuildmat.2017.05.146>
46. Poupelloz E, Gauffinet S, Nonat A (2020) Study of nucleation and growth processes of ettringite in diluted conditions. *Cem Concr Res* 127:105915. <https://doi.org/10.1016/j.cemconres.2019.105915>
47. Starinieri V, Hughes DC, Gosselin C et al (2013) Pre-hydration as a technique for the retardation of Roman cement mortars. *Cem Concr Res* 46:1–13. <https://doi.org/10.1016/j.cemconres.2013.01.004>
48. Ylmén R, Jäglid U (2013) Carbonation of portland cement studied by diffuse reflection Fourier transform infrared spectroscopy. *Int J Concr Struct Mater* 7:119–125. <https://doi.org/10.1007/s40069-013-0039-y>
49. Yaseen SA, Yiseen GA, Li Z (2019) Elucidation of calcite structure of calcium carbonate formation based on hydrated cement mixed with graphene oxide and reduced graphene oxide. *ACS Omega* 4:10160–10170. <https://doi.org/10.1021/acsomega.9b00042>
50. Pereira MA, Vasconcelos DCL, Vasconcelos WL (2019) Synthetic aluminosilicates for geopolymer production. *Mater Res* 22. <https://doi.org/10.1590/1980-5373-mr-2018-0508>

51. Elsen J (2006) Microscopy of historic mortars—a review. *Cem Concr Res* 36:1416–1424. <https://doi.org/10.1016/j.cemconres.2005.12.006>
52. Divya Rani S, Santhanam M, Bais S (2019) Historic incised plasterwork of India—characteristics and microstructure. *Constr Build Mater* 221:253–262. <https://doi.org/10.1016/j.conbuildmat.2019.06.057>
53. Pachta V, Goulas D (2020) Fresh and hardened state properties of fiber reinforced lime-based grouts. *Constr Build Mater* 261:119818. <https://doi.org/10.1016/j.conbuildmat.2020.119818>
54. de Azevedo ARG, Marvila MT, Tayeh BA et al (2021) Technological performance of açai natural fibre reinforced cement-based mortars. *J Build Eng* 33:101675. <https://doi.org/10.1016/j.jobe.2020.101675>
55. Marvila MT, Azevedo ARG, Cecchin D et al (2020) Durability of coating mortars containing açai fibers. *Case Stud Constr Mater* 13:e00406. <https://doi.org/10.1016/j.cscm.2020.e00406>

Publisher's Note Springer Nature remains neutral with regard to jurisdictional claims in published maps and institutional affiliations.

Springer Nature or its licensor holds exclusive rights to this article under a publishing agreement with the author(s) or other rightsholder(s); author self-archiving of the accepted manuscript version of this article is solely governed by the terms of such publishing agreement and applicable law.